Computationally Efficient Methods for Incorporation of Spectral Priors in 3-D Optical Tomography

Subhadra Srinivasan, Brian W. Pogue, and Frederic Leblond

***Abstract*—Use of spectral priors in optical tomography has significantly improved accuracy and quality of images, when applied in two-dimensional (2-D) models. However, the size of the problem increases substantially when applied in 3-D. Two methods are presented here that make 3-D spectral imaging computationally feasible. The 'data-subset' approach uses a smaller subset of available measurements to reduce the size of the inverse problem. The basic principle consists of using a dynamic criterion to select optimal subsets that capture the major changes in the imaging domain. Additionally, the sensitivity matrix is analyzed and made sparse based on a suitable threshold. Sparse matrix storage further reduces the memory requirements (to 8% of full matrix) and provides less than 2% percent difference in quantification compared to use of full matrices in the image reconstruction.**

I. Introduction

The relative transparency of biological tissues to near infra-red (NIR) light(low absorption from hemoglobin and water) allows penetration of photons through up to a dozen centimeters. This is the basis of optical imaging, which provides functional information through images of total hemoglobin, oxygen saturation and water that directly relates to the vascular and metabolic status of the tissue. NIR Imaging uses frequency domain or time domain measurements of light reflectance/transmittance at tissue boundaries to separate absorption and scattering properties with a suitable model for light propagation[1-3]. Prior knowledge of the primary absorbers or chromophores in the tissue along with multi- wavelength measurements leads to individual chromophore concentrations[4].

This imaging modality has a unique niche in diagnosis of breast cancer. Current breast imaging modalities such as mammography and MRI suffer from high false positive rates[5] and rely on structural features of tumors rather than functional information for diagnosis. Malignancies have higher hemoglobin due to angiogenesis and lower oxygenation due to high consumption. This provides the high intrinsic contrast potentially available through NIR tomography by imaging these absorbers[6, 7]. In addition, scattering provides structural information relating to the composition of the tissue[8, 9].

The spatial resolution of optical imaging is limited by the dominance of scattering over absorption[3, 10] making image reconstruction a difficult problem with a cost on the quantitative accuracy that cannot be overcome without prior information regarding the imaging domain. A major improvement in accuracy of optical images occurred with the incorporation of spectral priors that implements the expected spectral shapes of the chromophore and scattering models into the image formation process[11-13]. The approach uses simultaneously all available wavelengths of boundary data and incorporates the Beer's law for absorption and an empirical approximation to Mie theory for scattering[14, 15] as constraints. This reduces the solution space as well as the number of parameters to be reconstructed for and hence creates a more robust and stable algorithm. Applied in 2-D studies using continuous wave[11, 12], and frequency domain[13] data, results show reduced inter-parameter cross-talk and higher stability of the reconstruction to noise in measurements.

Our aim is to apply spectral priors in a 3-D model for light propagation, to extend the benefits of this approach to 3-D. However, 3-D spectral imaging faces a set of challenges due to the nature of the formulation of reconstruction problem. Multi-wavelength measurements used simultaneously quickly translate to large vectors for the imaging geometry under consideration. Additionally, reconstructing for multi-parameters (chromophore concentrations and scatter parameters) directly along with the large mesh sizes in 3-D quickly complicate the problem with huge memory requirements for inversion (ten times that for the conventional method without priors in a typical setting). Some of the approaches to deal with large computational problems involve a sub-zone type approach[16] or approximation of the mathematical formulation for inversion. The former method has difficulties dealing with boundaries that arise by approximating the 3-D volume into sub-zones which will result in loss of photons at the boundaries of the sub-zones. Schweiger et al[17] presented an alternate formulation for the Hessian in the Gauss-Newton setting, in order to exclude the explicit computation and storage of the Hessian. However, this method is not optimal in the current setting due to our large measurement data set.

We present here, alternate methods for applying spectral priors in 3-D. Specifically, we focus on a dynamic criterion

Manuscript received April 24, 2006. This work was funded by Advanced Research Technologies, ART Inc.

S. Srinivasan is with Dartmouth College, Thayer School of Engineering, Hanover, NH -03755, USA (phone: 603-646-2119; fax: 603-646-3856; e-mail: subha@dartmouth.edu).

B.W. Pogue is also with Dartmouth College, Thayer School of Engineering, Hanover, NH -03755, USA (e-mail: pogue@dartmouth.edu).

F. Leblond is with ART Inc., 2300 Alfred Nobel Blvd, Saint Laurent QC H4S ZA4 (e-mail: fleblond@art.ca).

to choose a subset of the available measurement set, which provides most information regarding the imaging domain. Use of this subset reduces the computational size of our problem significantly. In addition, we explore sparse matrix storage solutions in the frame-work of the 3-D spectral image reconstruction problem to reduce memory requirements and make the computation faster. We present results using these methods and future directions for methods with spectral priors.

II. METHODS

A. Imaging System

SoftScan™ is a time domain breast imaging clinical device developed by ART Advanced Research Technologies Inc. It was used as the imaging geometry in this study[18]. Figure 1(a) shows the system. The subject being imaged lies prostrate with the breast pendant; the breast fits into a rectangular box filled with an Intralipid matching liquid having optical properties similar to the breast tissue. A single source is raster scanned in step-and-shoot mode with a 3mm step size along the x and y directions; with five associated detector positions (see Fig. 1(b)) obtaining temporal point spread functions at four wavelengths in the NIR. Measurements on this geometry (mean time and intensity) were converted into frequency domain and a finite element model for diffusion approximation was used for image reconstruction. The diffusion approximation is used here because it holds for this detection geometry and tissue type where scattering dominates over absorption[19]. Details related to our finite element model can be found elsewhere[10, 20]. The theoretical framework for the incorporation of spectral priors has been explained in earlier references[13, 21].

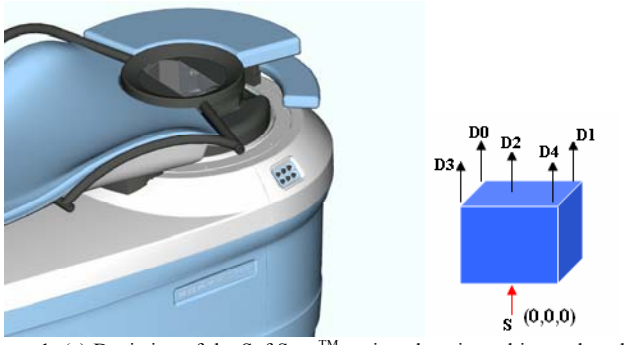

Figure 1: (a) Depiction of the SoftScan™, a time domain multi-wavelength breast imaging clinical device developed by ART Advanced Research Technologies Inc. (b) Source-detector geometry raster-scanned along the periphery of the rectangular slab containing the breast and an optical matching liquid.

B. Data subset Method

The main goal of the data subset method is to allow dealing with the large number of measurements encountered in breast diffuse optical tomography. The geometry described above yields ~10000 measurements (amplitude and phase) for a single wavelength on a typical breast sized domain. In the spectral method, multi-wavelength data are stacked together resulting in a total of ~40000 data points. The main assumption in this method is that because of redundancies not all measurements are required to reconstruct the key heterogeneities in the image. By separating the data points into lines and using a projection error criterion, a subset of the data is dynamically chosen. The projection error (χ^2) is the least squares functional being minimized in the image reconstruction,

$$\chi^2 = \sum_{j=1}^{M} \left(\Phi_{meas}^{j} - \Phi_{cal}^{j} \right)^2$$

where M is the total number of measurements in a single line, Φ_{meas} is the measured data and Φ_{cal} is the calculated data from the model. By starting with a homogeneous domain with background properties close to true values, and calculating χ^2, we obtain the error for individual lines of data. Using only those lines having maximum error and hence, maximum effect on the reconstruction, we reconstructed images for oxyhemoglobin, de-oxyhemoglobin, water and scatter parameters. The latter correspond to the scatter amplitude A and scatter power b which are governed by the spectral constraint $\mu_s'(\lambda) = A\lambda^{-b}$ where μ_s' is the reduced scattering coefficient as a function of wavelength λ [14, 22].

C. Sparse Matrix Storage Methods

The raster-scanning imaging geometry has some built-in advantages. One key aspect relating to this governs the sensitivity matrix. The sensitivity matrix holds the values for sensitivity of the boundary data (amplitude and phase) to local changes in chromophore concentrations and scattering. The sensitivity matrix has a banana-shape due to the diffusive nature of light, along the path of propagation from source to detector; and the values reduce quickly for nodes further away from this path. Hence, by setting a threshold based on this distance, and equating all values in the matrix below this threshold to zero, we can make the matrix sparse. Sparse matrix storage has much lesser memory requirements, and this eases the computational burden of the problem. This approach was implemented in the framework of the data subset approach. Inversion was carried out for both methods using a Gauss Newton method with Levenberg Marquardt regularization[10]. The stopping criterion for the image reconstruction was when projection error change between successive iterations was less than 2% of previous iteration error.

III. RESULTS

A. Projection error criterion

The data subset method was applied to data generated by the finite element model on a test phantom containing a single inclusion of size 15×15×20 mm centered at (30,30,30) mm in a rectangular slab of size 96×96×60mm, with 4:1 contrast in oxyhemoglobin. Figure 2 shows the

projection error for different lines of data along the x-axis in 3 mm resolution; each line has the source raster-scanned along the y-axis. The maximum error corresponds to slice 10, where the inclusion was centered. The projection error was used to select only 3 lines of data having maximum error, for image reconstruction, and the inclusion was recovered in the right location. Overall, the data subset method yielded less than 4% difference in quantification, compared to use of all available data, as tested on multiple phantoms[23].

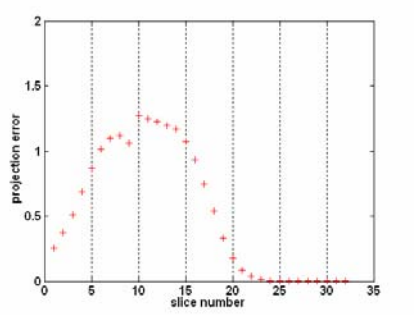

Figure 2: plot of the projection error for different lines (slices) of data in the case of a test phantom containing an inclusion centered at 30mm along the x axis. The maximum corresponds to the location of the inclusion. Only those lines with higher projection error were chosen for image reconstruction.

B. Sensitivity Matrix Storage

Shown in Figure 3(a) is a 3-D image of the matrix containing the sensitivity of logarithm of amplitude data to change in absorption coefficient, for a single measurement pair. Only the nodes close to the measurement pair have information significant to the image reconstruction. A threshold was set having the average of the matrix values, individually for each chromophore and each wavelength measurements and values below this threshold were set to zero. Figure 3(b) shows the sparsity pattern of the matrix, and the number of non-zero entries of this sparse matrix was only 8% of the full matrix.

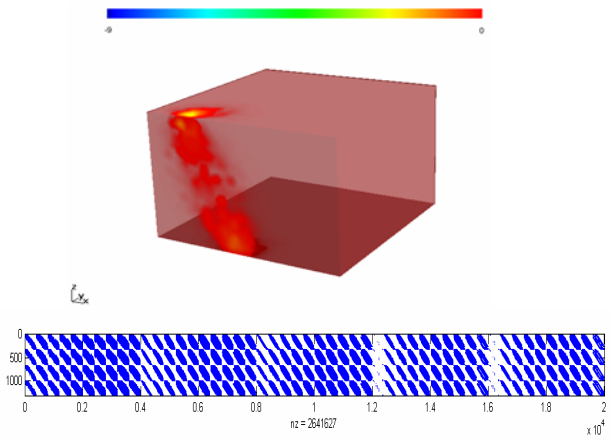

Figure 3: (a) sensitivity matrix plotted as a 3-D image for a single source-detector pair. Values for nodes away from the measurement are close to zero and do not have a significant impact in the inversion. (b) Sparsity pattern of the whole sensitivity matrix (for all chromophores, scatterers and wavelengths); making the matrix sparse reduces the number of non-zero entries to 8% of the full matrix.

Figure 4 shows a comparison of reconstructed images for oxyhemoglobin using the data subset approach and implementing the sensitivity threshold with sparse matrix storage. Both results were comparable with less than 2% difference in quantification for all reconstructed parameters .

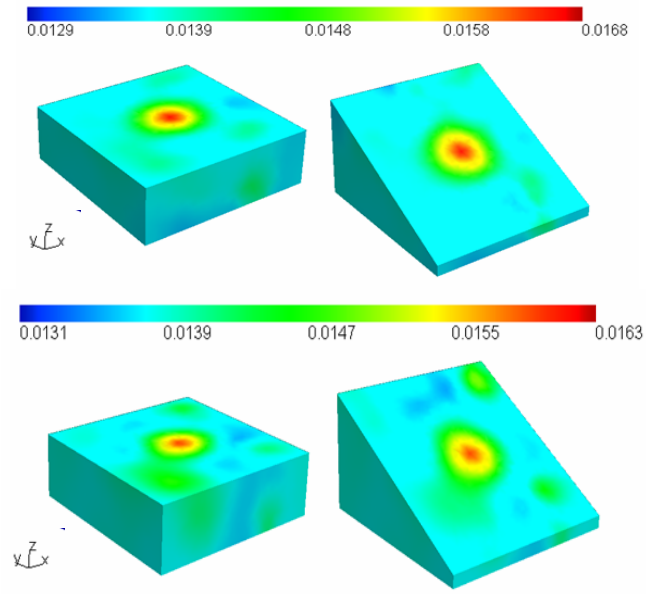

Figure 4: top row shows two cross-sections from the reconstructed 3-D oxyhemoglobin image obtained using data subset method without sparse matrix storage; bottom row shows corresponding results using a sparse sensitivity matrix with reduced memory requirements, obtained using thresholds as described.

IV. DISCUSSION

In the application of spectral priors to 3-D optical tomography computational resources are often pushed to their limits. All simulations carried out here were performed in a high-end multi-processor cluster, containing up to 16 gigabytes of memory. Yet, without the data subset method, spectral priors were not feasible in 3-D for reasonable breast mesh volumes. As 3-D optical imaging expands, research related to alternate computationally-efficient methods for image reconstruction is necessary. Two such methods were presented here.

The data subset approach indicates that the use of a subset of measurements providing most information regarding the imaging domain may be sufficient in image reconstruction. Additionally in the data subset method framework the sensitivity matrix stored as a sparse matrix reduced the memory needed to 8% of the full matrix without significant cost on accuracy.

The spectral approach holds considerable promise in accurate functional and structural imaging from optical tomography. It is desirable in increase the number of interrogation wavelengths in order to sample accurately changes due to different chromophores. Hence, the computational cost associated with using more wavelengths has to be optimized. Spatial priors from another modality

such as MRI can further reduce the burden by incorporation of anatomical structure to aid multi-region fitting. In this approach, the information relating to location of different tissue types such as adipose, fibro-glandular and tumor will be used along with spectral priors to reconstruct homogeneous functional and structural average values for each of the regions.

It is important to re-examine the assumptions behind spectral priors, namely that the principal absorbers and their spectra are known and that scattering can be approximated using an empirical power-law[14, 15]. Calibration of optical spectra specific to the imaging system helps optimize the accuracy relating to the first assumption[24]. The assumption regarding scattering has to be investigated further[25]. Additionally, differences in spectra for liquid surrounding the breast tissue have been taken into account for clinical subjects using prior knowledge of tissue boundary. In the future, possibilities of spectral changes in necrotic tissue present in some cancers could be studied and incorporated into the image reconstruction.

ACKNOWLEDGMENT

The authors thank Dr. Hamid Dehgani for his assistance with NIRFAST and Dr. Keith Paulsen for his insight in 3-D imaging problems. The authors would also like to thank Dr. Xavier Intes for his input.

REFERENCES

[1] M.S. Patterson, C. B., and B.C. Wilson, "Time resolved reflectance and transmittance for the non-invasive measurement of tissue optical properties." *Appl. Opt.*, vol. 28 pp. 2331-2336.1989.

[2] M.S. Patterson, Moulton, J. D., Wilson, B. C., Berndt, K. W., Lakowicz, J. R., "Frequency-domain reflectance for the determination of the scattering and absorption properties of tissue." *Appl. Opt.*, vol. 30(24) pp. 4474-4476.1991.

[3] S.R. Arridge and M. Schweiger, "Image reconstruction in optical tomography." *Phil. Trans. R. Soc. Lond. B*, vol. 352 pp. 717-726.1997.

[4] J.-L. Boulnois, "Photophysical processes in recent medical laser developments: a review." *Lasers in Medical Science*, vol. 1 pp. 47-66.1986.

[5] J.G. Elmore, M. B. Barton, V. M. Moceri, S. Polk, P. J. Arena and S. W. Fletcher, "Ten-Year Risk of False Positive Screening Mammograms and Clinical Breast Examinations." *The New England Journal of Medicine*, vol. 338(16) pp. 1089-1096.1998.

[6] B.W. Pogue, S.P. Poplack, T.O. McBride, W.A. Wells, O.K. S., U.L. Osterberg, and K.D. Paulsen, "Quantitative Hemoglobin Tomography with Diffuse Near-Infrared Spectroscopy: Pilot Results in the Breast." *Radiology*, vol. 218(1) pp. 261-6.2001.

[7] B.J. Tromberg, N. Shah, R. Lanning, A. Cerussi, J. Espinoza, T. Pham, L. Svaasand, and J. Butler, "Non-invasive in vivo characterization of breast tumors using photon migration spectroscopy." *Neoplasia (New York)*, vol. 2(1-2) pp. 26-40.2000.

[8] M.K. Simick, R. Jong, B. Wilson, and L. Lilge, "Non-ionizing near-infrared radiation transillumination spectroscopy for breast tissue density and assessment of breast cancer risk." *Journal of Biomed Opt*, vol. 9(4) pp. 794-803.2004.

[9] S. Srinivasan, B.W. Pogue, S. Jiang, H. Dehghani, C. Kogel, S. Soho, J.J. Gibson, T.D. Tosteson, S.P. Poplack, and K.D. Paulsen, "Interpreting hemoglobin and water concentration, oxygen saturation and scattering measured in vivo by near-infrared breast tomography." *PNAS*, vol. 100(21) pp. 12349-12354.2003.

[10] K.D. Paulsen, and Jiang H., "Spatially varying optical property reconstruction using a finite element diffusion equation approximation." *Med. Phys.*, vol. 22(6) pp. 691-701.1995.

[11] A. Corlu, T. Durduran, R. Choe, M. Schweiger, E.M. Hillman, S.R. Arridge, and A.G. Yodh, "Uniqueness and wavelength optimization in continuous-wave multispectral diffuse optical tomography." *Opt Lett*, vol. 28(23) pp. 2339-41.2003.

[12] A. Li, Q. Zhang, J.P. Culver, E.L. Miller, and D.A. Boas, "Reconstructing chromosphere concentration images directly by continuous-wave diffuse optical tomography." *Opt Lett*, vol. 29(3) pp. 256-8.2004.

[13] S. Srinivasan, Pogue, B. W., Jiang, S., Dehghani, H. and Paulsen, K. D., "Spectrally constrained chromophore and scattering NIR tomography provides quantitative and robust reconstruction." *Applied Optics*, vol. 44(10) pp. 1858-69.2005.

[14] H.J. van Staveren, C.J.M. Moes, J. van Marle, S.A. Prahl, and J.C. van Gemert, "Light scattering in Intralipid - 10% in the wavelength range of 400-1100nm." *Applied Optics*, vol. 30(31) pp. 4507-4514.1991.

[15] J.R. Mourant, T. Fuselier, J. Boyer, T.M. Johnson, and I.J. Bigio, "Predictions and measurements of scattering and absorption over broad wavelength ranges in tissue phantoms." *Applied Optics*, vol. 36(4) pp. 949-957.1997.

[16] M.J. Eppstein, D.E. Dougherty, D.J. Hawrysz, and E.M. Sevick, "Three-dimensional bayesian optical image reconstruction with domain decomposition." *IEEE Trans Med Imaging*, vol. 20(3) pp. 147-162.2001.

[17] M. Schweiger, S.R. Arridge, and I. Nissila, "Gauss-Newton method for image reconstruction in diffuse optical tomography." *Phys Med Biol*, vol. 50 pp. 2365-2386.2005.

[18] X. Intes, S. Djeziri, Z. Ichalalene, N. Mincu, Y. Wang, P. St-Jean, F. Lesage, D. Hall, D. Boas, M. Polyzos, P. Fleiszer, and B. Mesurolle, "Time-Domain Optical Mammography SoftScan: Initial Results." *Acad. Radiology*, vol. 12(8) pp. 934-947.2005.

[19] M.S. Patterson, B.C. Wilson, and D.R. Wyman, "The propagation of optical radiation in tissue II. Optical properties of tissues and resulting fluence distributions." *Lasers Med. Sci.*, vol. 6 pp. 379-390.1990.

[20] H. Dehghani, B.W. Pogue, J. Shudong, B. Brooksby, and K.D. Paulsen, "Three-dimensional optical-tomography: resolution in small-object imaging." *Applied Optics*, vol. 42(16) pp. 3117-3128.2003.

[21] B. Brooksby, S. Srinivasan, S. Jiang, H. Dehghani, B.W. Pogue, and K.D. Paulsen, "Spectral-prior information improves Near-Infrared diffuse tomography more than spatial-prior." *Optics Letters*, vol. 30(15) pp. 1968-70.2005.

[22] J.R. Mourant, T. Fuselier, J. Boyer, T.M. Johnson, and I.J. Bigio, "Predictions and measurements of scattering and absorption over broad wavelength ranges in tissue phantoms." *Applied Optics*, vol. 36(4) pp. 949.1997.

[23] S. Srinivasan, B.W. Pogue, H. Dehghani, F. Leblond, and X. Intes, "A Data Subset Algorithm for Computationally Efficient Reconstruction of 3-D Spectral Imaging in Diffuse Optical Tomography." *Optics Express*.2006-Submitted.

[24] S. Srinivasan, B.W. Pogue, S. Jiang, H. Dehghani, and K.D. Paulsen, *Validation of hemoglobin and water molar absorption spectra in near-infrared diffuse optical tomography*. Optical Tomography and Spectroscopy of Tissue V: Proceedings of SPIE, ed. B. Chance, et al. Vol. 4955. 2003. 407-415.

[25] X. Wang, B.W. Pogue, S. Jiang, X. Song, K.D. Paulsen, C. Kogel, S.P. Poplack, and W.A. Wells, "Approximation of Mie scattering parameters in near-infrared tomography of normal breast tissue in vivo." *Journal of Biomed Opt*, vol. 10(5) pp. 051704-1:051704-8.2005.